Thermally reduced graphite oxide as positive electrode in vanadium redox flow batteries

Zoraida González, Cristina Botas, Patricia Álvarez, Silvia Roldán, Clara Blanco[*]*, Ricardo Santamaría, Marcos Granda, and Rosa Menéndez*

Instituto Nacional del Carbón (INCAR-CSIC) Aptdo. 73, 33080-Oviedo, Spain

Abstract

Two graphene-like materials, obtained by thermal exfoliation and reduction of a graphite oxide at 700 and 1000ºC, were studied as active electrodes in the positive half-cell of a Vanadium Redox Flow Battery (VRFB**)**. In particular, that obtained at 1000ºC exhibited an outstanding electrochemical performance in terms of peak current densities (30.54 and 30.05 $mAcm^{-2}$ for the anodic and cathodic peaks at 1 mVs^{-1}, respectively) and reversibility (ΔE_p = 0.07 V). This excellent bahaviour is attributed to the restoration of sp^2 domains after thermal treatment, which implies the production of a graphene-like material with a high electrical conductivity and accessible surface area. Moreover, the residual functional groups, -OH, act as active sites towards the vanadium redox reactions. This represents a significant step forward in the development of highly effective VRFB electrode materials.

[*] Corresponding author: Fax: +34 985 29 76 62. E-mail address: clara@incar.csic.es (C. Blanco)

1. Introduction

The need to cover the rising energy demand has led to an increase in interest in electrochemical energy storage systems, among which Redox Flow Batteries (RFBs) have gained in importance. Unlike other types of batteries, the charge/discharge reactions associated with the battery operation are entirely related to chemical changes in the electroactive species dissolved in two solutions [1]. Thus, these batteries offer considerable advantages: a long life, a flexible design, a high energy efficiency (~ 70 %), as well as a low maintenance cost [2]. Vanadium Redox Flow Batteries (VRFBs), using the same metal in both half-cells [V(IV)/V(V) as the positive electrolyte and V(II)/V(III) as the negative one], additionally eliminate the shortcoming of cross-contamination characteristic of other secondary batteries [3].

The electrodes play an important role in VRFBs because, although they do not directly act as storage elements, they support the chemical reactions behind the battery operation. Consequently, choosing suitable electrode materials is of fundamental importance for obtaining a battery with a good performance. The materials must have a high electrical conductivity, a high mechanical strength, a good stability in the electrolyte and electrochemical activity [4]. Early studies made use of metals as electrodes in both half-cells of the battery, but their high cost and active-surface passivation made it necessary to search for alternative materials [5]. Carbon forms, such as graphite felts [6], carbon cloths [7] and carbon fibers [8] appeared as promising materials as they offered high specific surface areas at a reasonable cost. However, their low electrochemical activity due to poor kinetics and reversibility restricted their use as active electrodes. For this reason a great deal of effort has been directed to enhancing the electrochemical properties of these materials. Thermal [9], acidic [10] and galvanic [11] treatments, together with the deposition of metallic particles [12] on carbon surfaces, have all been investigated. However, the use of noble metals and the

tedious preparation procedures involved make these modified carbons less attractive for commercial applications. Thus, there is a clear need for new electrode materials.

In this context, the isolation of graphene in 2004 [13] represented a breakthrough for the scientific community. This two-dimensional one-atom-thick planar sheet of sp^2 bonded carbon atoms [14] possesses unique physical, chemical and thermal properties [15]. Among them, a high electrical conductivity, a high surface area, a widely applicable electrochemical activity and its relatively low production costs make graphene an ideal material for use in greener and more energy-efficient storage/generation devices such as supercapacitors [16], lithium-ion batteries [17] or fuel cells [18]. Despite the increase interest in graphenes for electrochemical applications, the use of these materials as electrodes in VRFBs has still not been widely investigated. So far, only a small number of studies have been published, most of them related to graphene oxide nanoplatelets (GONPs) [19].

In the present study, we investigate the suitability of two graphene-like materials obtained by thermal exfoliation and reduction of a graphite oxide (GO) to act as positive electrodes in a VRFB. The electrochemical behavior towards the V(IV)/V(V) redox reactions is explained from the structural and chemical characteristics of the materials.

2. Experimental

2.1 *Thermal exfoliation and reduction of GO*

GO was obtained by the oxidative treatment of a commercial graphite (powder, ‹ 20 μm, Aldrich) using a modified Hummers method [20]. This method makes use of the Hummers reagents with additional amounts of $NaNO_3$ and $KMnO_4$. Concentrated H_2SO_4 (360 mL) was added to a mixture of graphite (7.5 g) and $NaNO_3$ (7.5 g), and the mixture was cooled down to 0 °C using an ice bath. $KMnO_4$ (45 g) was added slowly in small doses to keep the reaction temperature below 20 °C. The solution was heated to 35 °C and stirred for 3 h, at this point 3 % of H_2O_2 (1.5 L) was added slowly, giving rise to a pronounced exothermal effect up to

98 °C. The reaction mixture was stirred for 30 min and then was centrifuged (3700 rpm for 30 min), the supernatant being decanted away. The remaining solid material was washed with 600 mL of water and centrifuged again, this process being repeated until the pH was neutral. GO was then thermally exfoliated and reduced in a tubular furnace under N_2 flow (100 mL min^{-1}) to 700 and 1000 ºC (5 ºC min^{-1}), to obtain two graphene-like materials labeled as TRG700 and TRG1000, respectively.

2.2 *Characterization of TRGs.*

The surface morphology of the samples was studied by SEM (using a FEI model Quanta FEG 650 instrument operating at 5 KV) and TEM (on a JEOL 2000 EX-II). XRD data were obtained using a Bruker D8 Advance diffractometer: the radiation frequency was the Kα1 line from Cu (1.5406 Å), operating at 40 KV and 40 mA. Raman spectra were recorded, from 750 to 3500 cm^{-1}, on a Renishaw 2000 Confocal Raman Microprobe (Rhenishaw Instruments, England) using a 514.5-nm argon ion laser. The apparent BET surface areas were determined by applying the BET equation to the nitrogen adsorption isotherms obtained at 77 K on a Micromeritics ASAP® 2420 instrument. The electrical conductivity of the samples was measured (at 20 MPa) using a modification of the four-probe method of Van der Pauw [21].

The total oxygen content of the samples was determined directly in a LECO-TF-900 furnace coupled to a LECO-CHNS-932 microanalyzer. The atomic oxygen content on the surface was determined by XPS analysis in a VG-Microtech Multilab 3000 spectrometer (SPECS, Germany) equipped with a hemispherical electron analyser and a MgKα ($h\nu$ = 1253.6 eV) X-ray source. Curve fitting of the C1s spectra was performed using a Gaussian-Lorentzian peak shape after performing a Shirley background correction.

2.3 *Electrochemical characterization*

Cyclic voltammetry experiments were performed in a Swagelok® type three-electrode cell at room temperature. The cell consisted of samples of GO, TRG700 or TRG1000, as the working electrode, Hg/Hg_2SO_4 as the reference electrode and platinum gauze as the counter electrode. The working electrodes were shaped like disks with a geometric surface area of 0.5 cm^2, containing 70 wt% of active material and 30 wt% of polyvinylidene fluoride as binder, and were dried in a vacuum oven at 110 ºC overnight before each experiment. All the potentials in this study are quoted with reference to Hg/Hg_2SO_4 (i.e, 0.65 V vs. ENH). The positive electrolyte consisted of a solution of 0.5 M $VOSO_4$ (Sigma Aldrich) in 1.0 M H_2SO_4 (VWR International). Electrochemical measurements were performed on a Biologic VMP Multichannel Potentiostat. The potential sweeps always started from the open circuit potential (OCP), the initial scan direction being positive. The scan rate, v_{scan}, was varied from 1 to 5 mVs^{-1}.

3. Results and discussion

3.1 *Structural, chemical and physical characteristics*

The thermal treatment of the GO at high temperatures (700 and 1000 ºC) generates graphene-like sheets (labelled TRG700 and TRG1000, respectively) which retain the typical shape of corrugated graphene layers, especially in the case of TRG700, as a result of thermal stabilization via bending (Figure 1a and c**)** [22]. These randomly aggregated sheets form disordered solids. TRG700 displays some regions with honeycomb structure due to a non complete exfoliation of the graphite. Meanwhile, TRG1000 has been fully exfoliated showing a wrinkle configuration (Figure 1b and d) [23], with smaller BET surface areas (Table 1**)** (271 and 97 m^2g^{-1} for TRG700 and TRG1000, respectively).

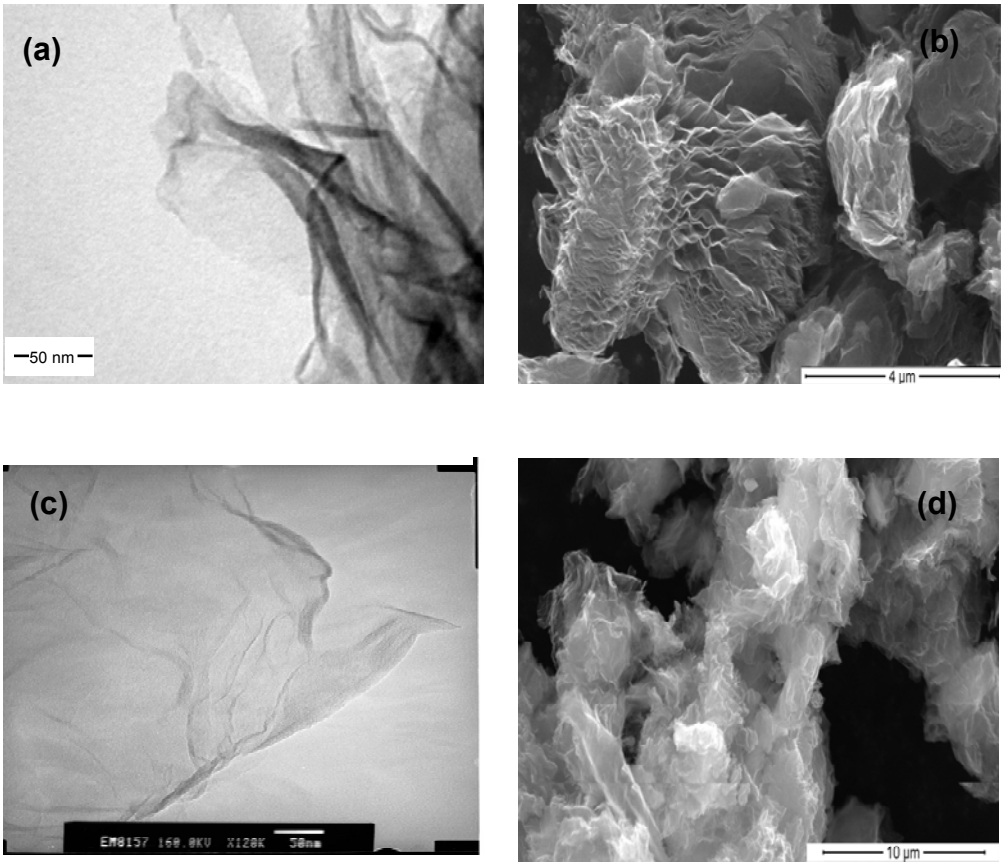

Figure 1. Microscopy images showing various morphologies: (a) TEM and (b) SEM images of TRG700; (c) TEM and (d) SEM images of TRG1000.

The structural changes that occurred during the thermal reduction process were followed by XRD and Raman spectroscopy (Table 1).

Table 1. Characteristics of GO and TRGs.

SAMPLE	Element. anal.	XPS	BET	RAMAN	XRD				Conductivity
	O (wt%)	O/C	S (m^2g^{-1})	I_D / I_G	2θ (º)	d (nm)	L_c (nm)	La (nm)	K (Scm^{-1})
GO	33,40	0,44	33	0,91	9,46	0,826	0,40	0,21	0,56
TRGO700	8,26	0,12	271	0,86	26,50	0,336	0,22	0,14	1,05
TRGO1000	1,91	0,10	97	1,17	24,55	0,362	0,16	0,50	2,12

Initially, the interlayer distance, *d*, changed from 0.338 nm, corresponding to the highly organized crystal structure of the graphite, to 0.826 nm of GO. This marked increase was caused by the incorporation of water and oxygen functional groups during the oxidation process [19]. The appearance of a D band in the Raman spectrum of the graphite oxide (Figure 2) and the high I_D/I_G ratio (0.91), corroborate the increasing disorder of the graphite layers [24]. After GO was heated to 700ºC, not only did the distance (0.336 nm for TRG700) decrease, but also the number of defects (I_D/I_G = 0.86) due to the removal of intercalated water and the decomposition of most of the oxygen functional groups [25]. The electrical conductivity of TRG700 (Table 1**)** increased significantly (up to 1.05 Scm^{-1}) due to the recovery of C=C bonds, which should lead to a better electrochemical behavior [26].

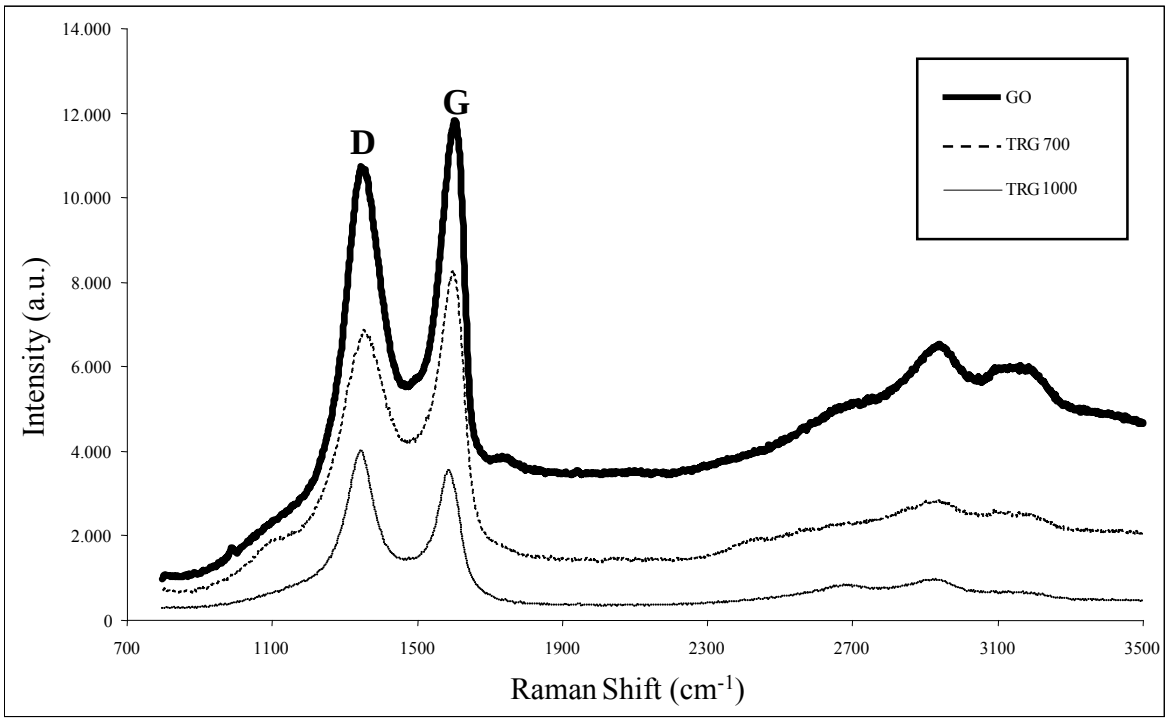

Figure 2**.** Raman spectra of GO, TRG700 and TRG1000.

When the thermal treatment temperature was increased to 1000 ºC, the structural parameters of TRG1000 interrupted their decreasing trend. A *d* value of 0.362 nm was recorded while the I_D/I_G ratio rose to 1.17. These results can be attributed to the effect of the temperature which caused a more pronounced decomposition of the oxygen functional groups, leading to graphene-like sheets with a greater number of edge planes and a disordered stacking [27,28] (see the corresponding SEM image in Figure 1). Moreover the sp^2 domains of each single-sheet were restored, yielding a higher electrical conductivity (2.12 Scm^{-1}), which should result in a better electrochemical performance of the electrode material.

These structural changes were accompanied by chemical changes which were evaluated by elemental and XPS analyses (Table 1). The oxygen content experienced a marked decrease with the thermal treatment from 33.40 % for GO to 8.26 % and 1.91 % for TRG700 and TRG1000, respectively. The O/C ratio decreased from 0.44 for GO to 0.12 and 0.10 for TRG700 and TRG1000, respectively. These results confirm the effectiveness of the thermal reduction in eliminating the oxygen functional groups incorporated during the oxidation treatment of the graphite [29]. In order to identify the residual oxygen functional groups, the C1s spectra of the samples were analyzed (Figure 3).

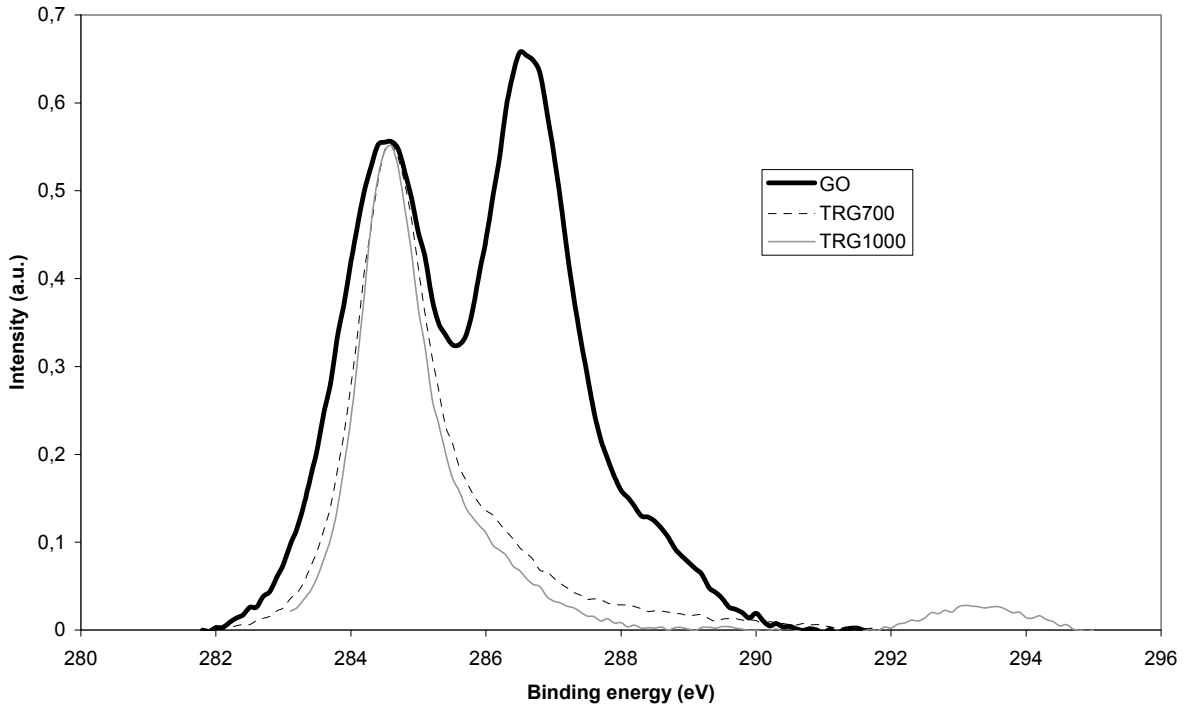

Figure 3**.** C1s XPS spectra of GO and TRGs.

The sharp rise of the sp^2 –hybridized carbon content (from 40.9 % for GO to 70.9 % and 74.5 % for TRG700 and TRG1000, respectively) and the π-π^* interaction (from 0.1% for GO to 0.8 % and 4.6% for TRG700 and TRG1000, respectively) (Table 2) confirm the results of the Raman analysis presented above. The peak assignments of the different functional groups showed that whereas TRG700 had similar amounts of C=O and C-OH groups, C-OH groups were predominant in TRG1000 [30].

Table 2**.** Functional groups provided by curve fitting of C1s spectra.

	GO (%)	TRG700 (%)	TRG1000 (%)
Csp2	40,9	70,9	74,5
Csp3	4,3	17,9	19,7
C-OH	27,3	5,4	2,1
C=O	21,8	4,0	0,9
O=C-OH	6,2	2,1	0,0
π-π*	0,1	0,8	4,6

3.2 *Electrochemical performance*

The suitability of the as characterized TRG700 and TRG1000 to act as positive electrodes in a VRFB was tested by Cyclic Voltammetry experiments (Figure 4). GO was included for comparative purposes.

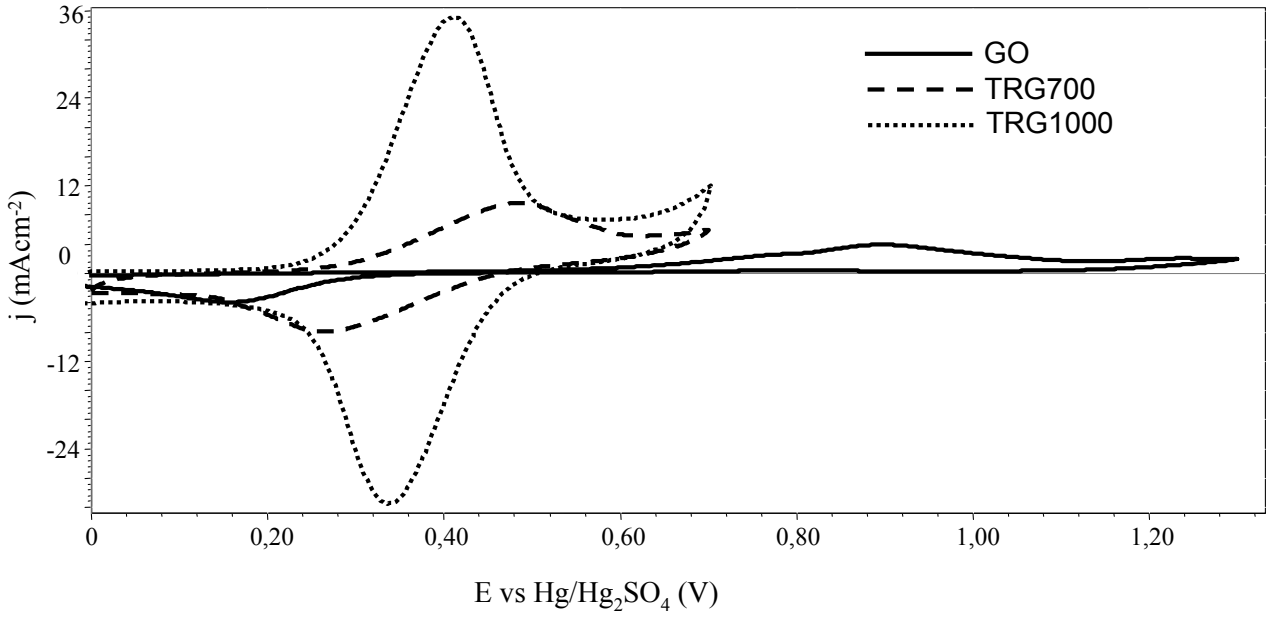

Figure 4. Cyclic Voltammograms (CVs) of V(IV)/V(V) on GO and TRGs recorded in a 0.5 M $VOSO_4$ / 1.0 M H_2SO_4 solution at a scan rate of 1 mVs^{-1}.

The three samples exhibit an anodic peak associated with the oxidation of V(IV) to V(V), and a cathodic one associated with the reverse reaction. However, there are significant differences in the measured peak potentials (E_{pa} and E_{pc}) and current densities (j_{pa} and j_{pc}) values, which reflect substantial differences in the electrochemical performance (Table 3).

Table 3. Electrochemical parameters obtained from the CVs (at 1 mVs^{-1}) for V(IV)/V(V) on the three tested samples.

	Anodic peak		Cathodic peak		
SAMPLE	**j_{pa} ($mAcm^{-2}$)**	**E_{pa} (V)**	**j_{pc} ($mAcm^{-2}$)**	**E_{pc} (V)**	**ΔE_p (V)**
GO	2,72	0,89	3,5	0,16	0,73
TRG700	6,3	0,48	6,84	0,27	0,21
TRG1000	30,54	0,41	30,05	0,34	0,07

In the case of GO, the peak potential separation (ΔE_p) of 0.73 V, corresponding to the vanadium redox reaction under study, indicates that GO is electrochemically irreversible on this type of electrode. TRG700 exhibits a better electrochemical activity, as the corresponding voltammogram shows a significant increase in peak current densities and a decrease in the ΔE_p (0.21 V) values, indicating that the electrochemical reaction is a quasi-reversible process on this type of electrode. This improved performance can be ascribed to the increase in the electrical conductivity experienced by this graphene-like material after the thermal reduction of GO at 700ºC.

However, the best results were obtained on TRG1000 (Figure 4). This electrode exhibits the highest anodic and cathodic peak current densities and the lowest ΔE_p (0.07V) values, reflecting the huge improvement in the electrochemical activity towards the V(IV)/V(V) redox reactions. Furthermore, repetitive CVs were performed (100 scans at 1 mVs^{-1}) and no significant changes in current densities or peak potential values were observed. This can be taken as an evidence of the long-term stability of this electrode, although flow battery tests will be needed to determine its stability in an operating system.

These higher values of j_{pa} and j_{pc}, together with the reversibility condition mentioned above, evidence that the TRG1000 electrode is the most appropriate material over the potential range studied. Thus, it is confirmed that this graphene-like material presents the structural, chemical and physical characteristics required for an active electrode material: not only does it have a higher electrical conductivity but also an accessible surface area with appropriate oxygen functional groups, which act as active sites for catalyzing the vanadium redox reactions [31]. It should be pointed out that these excellent results are not only better than those obtained with GONPs (e.g. the reversibility of the vanadium redox reactions is improved about 60 mV)

[19], but also they are comparable to the best previously published, results obtained on a metal-modified graphite felt as active electrode material in a VRFB [32].

In order to compare the V(IV)/V(V) redox processes on the TRGs electrodes, cyclic CVs were recorded at different scan rates (1, 2 and 5 mVs^{-1}), maintaining the rest of experimental conditions (Figure 5).

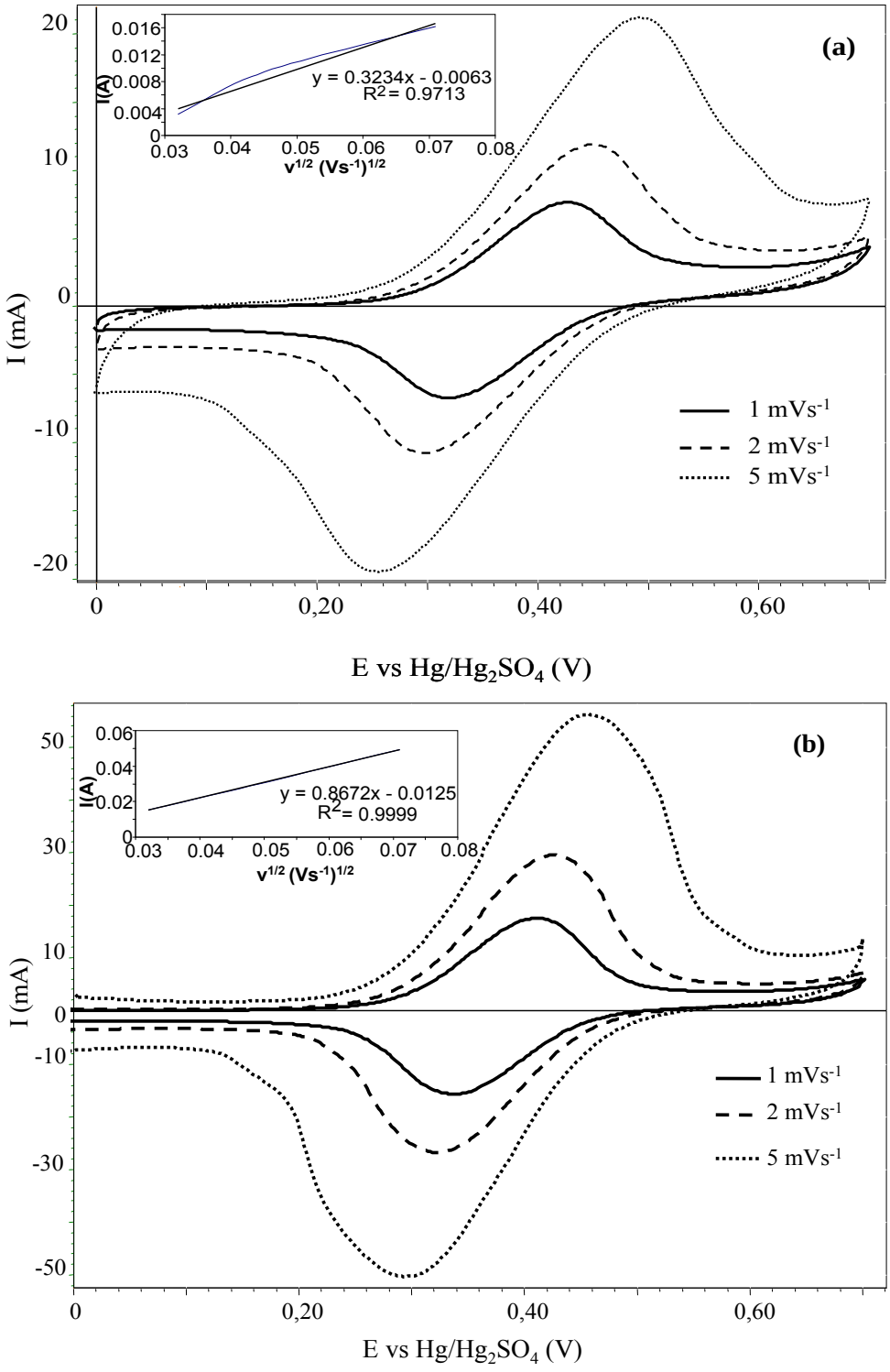

Figure 5**.** CVs recorded on (a) TRG700 and (b) TRG1000 electrodes, in a 0.5 M $VOSO_4$ / 1.0 M H_2SO_4 solution, at various scan rates.

In the two electrodes, the ΔE_p value increases with the scan rate, which could be explained taking into account their different polarization [33]. The polarization of TRG1000 is reduced significantly in comparison to that of TRG700, because of the higher electrical conductivity attained by the first one, which highly improves the charge transfer at the electrode/electrolyte interface. Furthermore, the linear relationship (R^2 = 0.9999) between the anodic peak currents and the square root of the scan rate only observed on TRG1000 indicates that the oxidation of the V(IV) specie might be only limited by its transport in the electrolyte in the range of scan rates tested [34], while on TRG700 (R^2 = 0.9713) this redox reaction might have a mixed control (charge transfer/ionic transport in the electrolyte).

4. Conclusions

Two graphene-like materials suitable for use as positive electrodes in a VRFB were obtained by thermal exfoliation and reduction of a graphite oxide. After thermal reduction, the electrocatalytic activity of TRG700 and TRG1000 towards the redox reactions associated to V(IV)/V(V) is markedly enhanced with respect to GO. In particular, TRG1000 exhibits an outstanding electrochemical performance in terms of peak current densities values (30.54 and 30.05 $mAcm^{-2}$ for the anodic and cathodic peaks at 1 mVs^{-1}, respectively) and reversibility, reaching a peak potential separation value, ΔE_p, of 0.07 mV. These excellent results are attributed to the restoration of sp^2 domains after thermal treatment, which implies the production of a graphene-like material with a high electrical conductivity and accessible surface area. Moreover, the residual functional groups, -OH, act as active sites towards the vanadium redox reactions. This represents a significant step forward in the development of highly effective VRFB electrode materials.

Acknowledgements

The authors thank MICINN (CONSOLIDER INGENIO 2010, Ref. CSD2009-00050 and MAT 2010-20601-C02-01), FICYT (Project PC10-35) and HC Energía. for their financial support. Dr. Patricia Alvarez thanks MICINN for her Ramon y Cajal research contract. Cristina Botas acknowledges a fellowship from FICYT. Silvia Roldán thanks MICINN for a FPI pre-doctoral research grant.

References

[1] Ponce de León C, Frías-Ferrer A, González-García J, Szánto DA, Walsh FC. Redox flow cells for energy conversion. J. of Power Sources 2006**;** 160: 716-732.

[2] Liu Q, Sleightholme A, Shinkle A, Li Y, Thompson LT. Non-aqueous vanadium acetylacetonate electrolyte for redox flow batteries. Electrochem. Commun. 2009; 11: 2312-2315.

[3] Bartolozzi M. Electrochemical performance of lithium/sulfur cells with three different polymer electrolytes. J. Power Sources 1989; 27: 219-226.

[4] Haddadi-Asl V, Kazacos M, Skyllas-Kazacos M. Conductive carbon-polypropylene composite electrodes for vanadium redox battery. J. Appl. Polymer Sci. 1995; 25: 29-33.

[5] Rychcik M, Skyllas-Kazacos M. Evaluation of electrode materials for vanadium redox cell.

J. Power Sources 1987; 19: 45-54.

[6] Zhong S, Paeste C, Skyllas-Kazacos M. Comparison of the physical, chemical and electrochemical properties of rayon- and polyacrylonitrile-based graphite felt electrodes. J. Power Sources 1993; 45(1): 29-41.

[7] Kaneko H, Nozaki K, Wada Y, Aoki T, Negishi A, Kamimoto M. Vanadium redox reactions and carbon electrodes for vanadium redox flow battery. Electrochim. Acta 1991; 36(7): 1191-1196.

[8] Kamarudin SK, Daud WRW, Ho SL, Hasran UA. Overview on the challenges and developments of micro-direct methanol fuel cells (DMFC). J. Power Sources 2007; 163(2): 743-754.

[9] Sun B, Skyllas-Kazacos M. Modification of graphite electrode materials for vanadium redox flow battery application—I. Thermal treatment. Electrochim. Acta 1992; 37: 1253-1260.

[10] Sun B, Skyllas-Kazacos M, Chemical modification of graphite electrode materials for vanadium redox flow battery application—part II. Acid treatments. Electrochim. Acta 1992; 37: 2459-2465.

[11] Li X, Huang K, Liu S, Tan N, Chen L. Characteristics of graphite felt electrode electrochemically oxidized for vanadium redox battery application. Trans. Nonferrous Mat. Soc. China 2007; 17: 195-199.

[12] Sun B, Skyllas-Kazacos M. Chemical modification and electrochemical behaviour of graphite fibre in acidic vanadium solution**.** Electrochim. Acta 1991; 36(3/4):513-517.

[13] Novoselov KS, Geim AK, Morozov SV, Jiang D, Zhang Y, Dubonos SV, Grigorieva IV, Firsov AA**.** Electric Field Effect in Atomically Thin Carbon Films. Science 2004; 306: 666-669.

[14] Geim AK, Novoselov KS. The rise of graphene. Nat. Mat. 2007; 6: 183-191.

[15] Chen D, Tang L, Li J. Graphene-based materials in electrochemistry. Chem. Soc. Rev. 2010; 39: 3157-3180.

[16] Wang Y, Shi Z, Huang Y, Ma Y, Wang C, Chen M, Chen Y. Supercapacitor Devices Based on Graphene Materials. J. Phy. Chem. C 2009; 113: 13103-13107.

[17] Yoo EJ, Kim J, Hosono E, Zhou HS, Kudo T, Honma I. Enhanced Cyclic Performance and Lithium Storage Capacity of SnO_2/Graphene Nanoporous Electrodes with Three-Dimensionally Delaminated Flexible Structure. Nano Lett. 2008; 8: 2277-2282.

[18] Qu L, Baek YJ, Dai L. Nitrogen-Doped Graphene as Efficient Metal-Free Electrocatalyst for Oxygen Reduction in Fuel Cells. ACS Nano 2010; 4: 1321-1326.

[19] Han P, Wang H, Liu Z, Chen X, Ma W, Yao J, Zhu Y, Cui G. Graphene oxide nanoplatelets as excellent electrochemical active materials for VO^{2+}/VO_2^{+} and V^{2+}/V^{3+} redox couples for a vanadium redox flow battery. Carbon 2011; 49: 693-700.

[20] Hummers WS, Offeman RE. Preparation of Graphitic Oxide. J. Am. Chem. Soc. 1958; 80: 1339.

[21] Van der Pauw LJ. A method of measuring the resistivity and Hall coefficient on Lamellae of arbitrary shape. Philips Tech. Rev. 1958; 20: 220-224.

[22] Meyer JC, Geim AK, Katsnelson MI, Novoselov KS, Booth TJ, Roth S. The structure of suspended graphene sheets. Nature 2007; 446: 60-63.

[23] McAllister MJ, Li J-L, Adamson DH, Schiepp HC, Abdala AA, Liu J, Herrera-Alonso M, Milius DL, Car R, Prud´homme RK, Aksay IA. Single Sheet Functionalized Graphene by Oxidation and Thermal Expansion of Graphite. Chem. Mater. 2007**;** 19: 4396-4404.

[24] Gómez-Navarro C, Weitz RT, Bittner AM, Scolari M, Mews A, Burghard M, Kern K. Electronic Transport Properties of Individual Chemically Reduced Graphene Oxide Sheets. Nano Lett. 2007; 7 (11): 3499-3503.

[25] Kudin KN, Ozbas B, Schniepp HC, Prudhomme RK, Aksay IA, Car R. Raman Spectra of Graphite Oxide and Functionalized Graphene Sheets. Nano Lett. 2008; 8(1): 36-41.

[26] Kang H, Kulkarni A, Stankovich S, Ruoff RS, Baik S. Restoring electrical conductivity of dielectrophoretically assembled graphite oxide sheets by thermal and chemical reduction techniques. Carbon 2009; 47: 1520-1525.

[27] Stankovich S, Dikin DA, Piner RD, Kohlhaas KA, Kleinhammes A, Jia Y, Wu Y, Nguyen ST, Ruoff RS. Synthesis of graphene-based nanosheets via chemical reduction of exfoliated graphite oxide. Carbon 2007; 45: 1558-1565.

[28] Mwakikunga BW, Sideras-Haddad E, Arendse C, Witcomb MJ, Forbes A. WO_3 nano-spheres into $W_{18}O_{49}$ one-dimensional nano-structures through thermal annealing. J. Nanosci. & Nanotechnol. 2009; 9: 3286-3294.

[29] Yang D, Velamakanni A, Bozoklu G, Park S, Stoller M, Piner RD, Stankovich S, Jung I, Field DA, Ventrice CA Jr., Ruoff RS. Chemical analysis of graphene oxide films after heat and chemical treatments by X-ray photoelectron and Micro-Raman spectroscopy. Carbon 2009; 47: 145-152.

[30] Gao X, Jang J, Nagase S. Hydrazine and Thermal Reduction of Graphene Oxide: Reaction Mechanisms, Product Structures, and Reaction Design. J. Phys. Chem. C 2010; 114: 832-842.

[31] Yue L, Li W, Sun F, Zhao L, Xing L. Highly hydroxylated carbon fibres as electrode materials of all-vanadium redox flow battery. Carbon 2010; 48: 3079-3090.

[32] Wang WH, Wang XD. Investigation of Ir-modified carbon felt as the positive electrode of an all-vanadium redox flow battery. Electrochim. Acta 2007; 52: 6755-6762.

[33] Li W, Liu J, Yan C. Graphite–graphite oxide composite electrode for vanadium redox flow battery. Electrochim. Acta 2011; 56: 5290-5294.

[34] Kim JH, Kim KJ, Park MS, Lee NJ, Hwang U, Kim H, Kim YJ. Development of metal-based electrodes for non-aqueous redox flow batteries. Electrochem, Commun, (2011), doi: 10.1016/j.elecom.2011.06.022

Table Captions

Table 1**.** Characteristics of GO and TRGs.

Table 2**.** Functional groups provided by curve fitting of C1s spectra.

Table 3. Electrochemical parameters obtained from the CVs (at 1 mVs^{-1}) for V(IV)/V(V) on the three tested samples.

Figure Captions

Figure 1. Microscopy images showing various morphologies**:** (a) TEM and (b) SEM images of TRG700; (c) TEM and (d) SEM images of TRG1000

Figure 2. Raman spectra of GO, TRG700 and TRG1000.

Figure 3. C1s XPS spectra of GO and TRGs

Figure 4. Cyclic Voltammograms (CVs) of V(IV)/V(V) on GO and TRGs recorded in a 0.5 M $VOSO_4$ / 1.0 M H_2SO_4 solution at a scan rate of 1 mVs^{-1}.

Figure 5. CVs recorded on (a) TRG700 and (b) TRG1000 electrodes, in a 0.5 M $VOSO_4$ / 1.0 M H_2SO_4 solution, at various scan rates

Supporting Information

Title Thermally reduced graphite oxide as positive electrode in vanadium redox flow batteries

Zoraida González, Cristina Botas, Patricia Álvarez, Silvia Roldán, Clara Blanco, Ricardo Santamaría, Marcos Granda, and Rosa Menéndez*

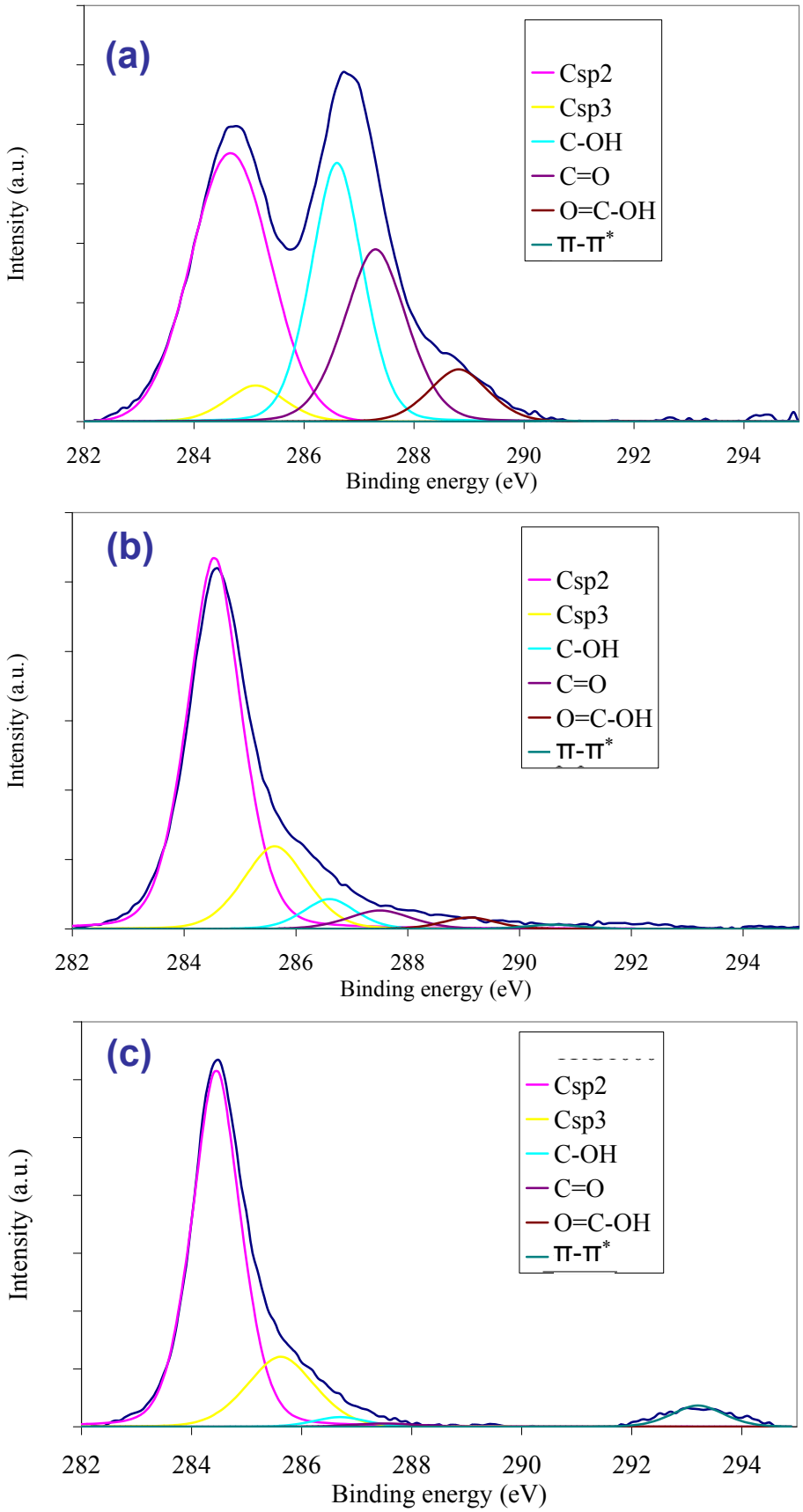

Figure S1. Curve fitting of C1s XPS spectra of (a) GO, (b) TRG700 and (c) TRG1000.

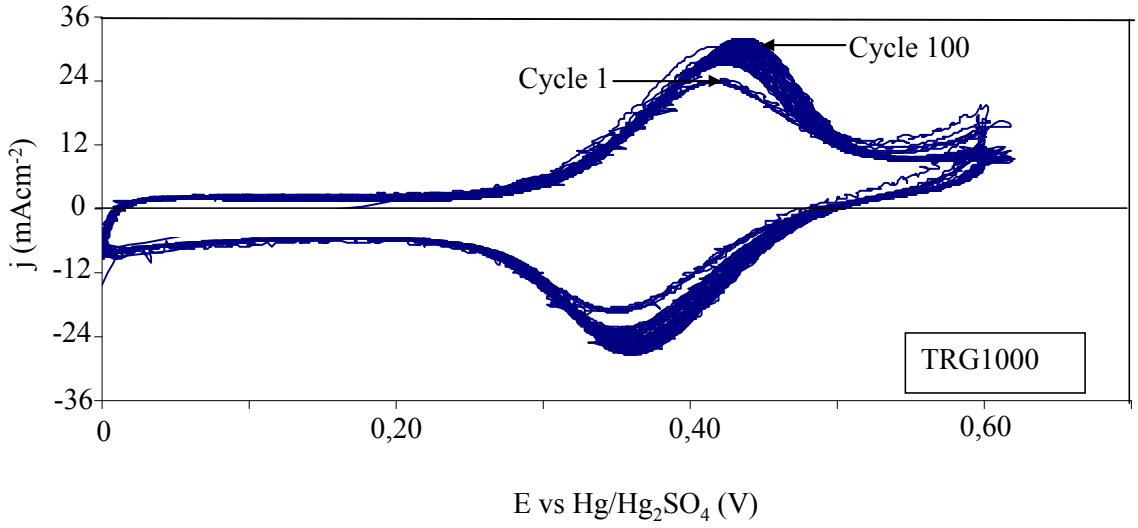

Figure S2. Repetitive cyclic voltammograms (100 scans) of V(IV)/V(V) on TRG1000 recorded in a 0.5 M $VOSO_4$ / 1.0 M H_2SO_4 solution at a scan rate of 1 mVs^{-1}.